Available online at www.sciencedirect.com
SCIENCE DIRECT
Biochemical Pharmacology 70 (2005) 1487–1496
Biochemical Pharmacology
www.elsevier.com/locate/biochempharm

Human adenosine A_3 receptor leads to intracellular Ca^{2+} mobilization but is insufficient to activate the signaling pathway via phosphoinositide 3-kinase γ in mice

Kazuya Yamano [a], Miho Inoue [a], Shigehiro Masaki [b], Mayumi Saki [b], Michio Ichimura [a], Mitsuo Satoh [a,*]

[a] *Tokyo Research Laboratories, Kyowa Hakko Kogyo Co. Ltd., 3-6-6 Asahi-machi, Machida-shi, Tokyo 194-8533, Japan*
[b] *Pharmaceutical Research Center, Kyowa Hakko Kogyo Co. Ltd., 1188 Shimotogari, Nagaizumi-cho, Sunto-gun, Shizuoka 411-8731, Japan*

Received 27 June 2005; accepted 10 August 2005

Abstract

Selective antagonists for the adenosine A_3 receptor (A3AR), a member of the G protein-coupled receptors, have been indicated as potential drugs for anti-asthma or anti-inflammation. However, potent antagonists for the rodent A3AR have not been identified. To evaluate the pharmacological effects of human A3AR antagonists in mice, we here generated A3AR-humanized mice, in which the mouse A3AR gene was replaced by its human counterpart. The expression levels of human A3AR in the A3AR-humanized mice were equivalent to those of mouse A3AR in wild-type mice. Elevation of the intracellular Ca^{2+} concentration induced by an A3AR agonist was observed in bone marrow-derived mast cells from the A3AR-humanized mice and this Ca^{2+} mobilization was completely antagonized by a human A3AR antagonist. However, antigen-dependent degranulation was not potentiated by the A3AR agonist in the mast cells from A3AR-humanized mice. The agonist-stimulated human A3AR did not lead to the phosphorylation of either extracellular signal-regulated kinase 1/2 or protein kinase B in A3AR-humanized mice. The rate of human A3AR internalization in the mast cells was also markedly decreased compared with that of mouse A3AR in the mast cells. These results demonstrate that the human A3AR is insufficient to activate phosphoinositide 3-kinase γ-dependent signaling pathways in mice, probably due to the uncoupling of member(s) of the G proteins, which are capable of activating phosphoinositide 3-kinase γ, to the human A3AR, despite the mouse G protein(s) responsible for the Ca^{2+} elevation are coupled with the human A3AR.

Keywords: Adenosine A_3 receptor; Phosphoinositide 3-kinase γ; $G_{i/o}$ protein; G protein-coupled receptor; Humanized mice; Species difference

1. Introduction

Adenosine physiologically acts through four G protein-coupled receptors (GPCRs), the A_1, A_{2A}, A_{2B}, and A_3 receptors [1–3]. The adenosine A_3 receptor (A3AR) is known to couple to some G proteins of the pertussis toxin-sensitive $G_{i/o}$ family [4,5]. The adenosine-bound A3AR induces βγ subunits release from the heterotrimeric $G_{i/o}$ proteins, and the α and βγ subunits regulate diverse cellular signaling pathways [6]. Some of the released βγ subunits lead to the mobilization of intracellular Ca^{2+} via the signal transducers, such as phospholipase C (PLC) β [6,7], and some others activate phosphoinositide 3-kinase (PI3K) γ, a class IB PI3K isoform [8]. PI3Kγ leads to the phosphorylation of protein kinase B (PKB), also referred to as Akt [4,9], and to the phosphorylation of members of the

Abbreviations: A3AR, adenosine A_3 receptor; $A3AR^{h/h}$ mice, A3AR-humanized mice; BMMCs, bone marrow-derived mast cells; $[Ca^{2+}]_i$, intracellular Ca^{2+} concentration; Cl-IB-MECA, 2-chloro-N^6-(3-iodobenzyl)adenosine-5′-*N*-methyluronamide; DT-A, diphtheria toxin A fragment; EPO, erythropoietin; ERK1/2, extracellular signal-regulated kinase 1/2; ES cells, embryonic stem cells; GPCR, G protein-coupled receptor; HAT, hypoxanthine/aminopterin/thymidine; HEK293 cells, human embryonic kidney 293 cells; HPRT, hypoxanthine phosphoribosyltransferase; [^{125}I]AB-MECA, N^6-(4-amino-3-[^{125}I]iodobenzyl)adenosine-5′-*N*-methyluronamide; KF26777, 2-(4-bromophenyl)-7,8-dihydro-4-propyl-1*H*-imidazo[2,1-*i*]purin-5(4*H*)-one dihydrochloride; MAPK, mitogen-activated protein kinase; MIP-1α, macrophage inflammatory protein-1α; PCR, polymerase chain reaction; PI3Kγ, phosphoinositide 3-kinase γ; PKB, protein kinase B; PLCβ, phospholipase C β; (*R*)-PIA, (*R*)-N^6-phenylisopropyladenosine; RANTES, regulated on activation of T cell expressed and secreted; RT-PCR, reverse transcription-PCR; TNP, 2,4,6-trinitrophenyl; anti-TNP IgE, monoclonal IgE antibody against 2,4,6-trinitrophenyl

* Corresponding author. Tel.: +81 42 725 2555; fax: +81 42 726 8330.
E-mail address: msatoh@kyowa.co.jp (M. Satoh).

0006-2952/$ – see front matter © 2005 Elsevier Inc. All rights reserved.
doi:10.1016/j.bcp.2005.08.003

mitogen-activated protein kinase (MAPK) family, including extracellular signal-regulated kinase (ERK) 1/2 [4] and stress-activated protein kinase p38 [10]. These phosphorylated proteins play important roles in cellular phenomena, such as cell proliferation, differentiation, and apoptosis [11–15]. In mast cells, PI3Kγ plays a key role in the potentiation of antigen/IgE-dependent mast cell degranulation by the A3AR [9].

Recently, the A3AR has attracted considerable interest as a novel drug target against cerebral/cardiac ischemia, cancer, and inflammation [16–18]. A number of studies using A3AR-deficient mice have suggested that the A3AR antagonists possess potential as drugs for the treatment of asthma and chronic obstructive pulmonary disease [19–21]. Thus, potent and selective antagonists for the human A3AR are screened and identified, whereas all of the human A3AR antagonists show extremely low binding affinity for the rodent A3AR (the K_i values of A3AR antagonists for the rodent A3AR are 1000 times lower than that for the human A3AR) and potent antagonists for the rodent A3AR has not been identified [16,17]. In general, animal studies using rodent models are essential for the evaluation of pharmacological effects of new therapeutic agents through the early preclinical stages of drug development. However, the large species differences between rodent and human A3AR and the lack of highly potent antagonists for the rodent A3AR are currently serious drawbacks in the further pharmacological evaluation of A3AR antagonists, yielding only a poor understanding of physiological function of the human A3AR [16,17].

In this study, we generated mice in which the A3AR gene was replaced by its human counterpart, A3AR-humanized ($A3AR^{h/h}$) mice, in order to evaluate the pharmacological effects of human A3AR antagonists in mouse models. The intracellular Ca^{2+} mobilization evoked by an A3AR agonist was antagonized by the human A3AR antagonist; however, unexpectedly, the activation of the PI3Kγ-dependent signaling pathway by the agonist-mediated A3AR was abolished in bone marrow-derived mast cells (BMMCs) from the $A3AR^{h/h}$ mice. Our findings suggest that the replacement of the A3AR gene with its human counterpart may be functionally insufficient to generate A3AR-humanized mice, probably due to the uncoupling between human A3AR and mouse G protein.

2. Materials and methods

2.1. Materials

N^6-(4-Amino-3-[^{125}I]iodobenzyl)adenosine-5′-*N*-methyluronamide ([^{125}I]AB-MECA, specific activity, 74 TBq/mmol) was purchased from Amersham (Buckinghamshire, UK). (*R*)-N^6-Phenylisopropyladenosine ((*R*)-PIA), adenosine deaminase, macrophage inflammatory protein-1α (MIP-1α), and regulated on activation of T cell expressed and secreted (RANTES) were obtained from SIGMA (St. Louis, MO). Rabbit anti-ERK1/2 antibody, rabbit anti-phospho ERK1/2 (Thr202/Tyr204) antibody, rabbit anti-PKB antibody, rabbit anti-phospho PKB (Ser473) antibody, and the Phototope HRP Western Blot Detection Kit were purchased from Cell Signals Technology (Beverly, MA). Fluo-3 AM was obtained from Molecular Probes (Eugene, OR). 2-Chloro-N^6-(3-iodobenzyl)adenosine-5′-*N*-methyluronamide (Cl-IB-MECA) and 2-(4-bromophenyl)-7,8-dihydro-4-propyl-1*H*-imidazo[2,1-*i*]purin-5(4*H*)-one dihydrochloride (KF26777) were synthesized in our laboratories. 2,4,6-Trinitrophenyl bovine serum albumin (TNP-BSA) was from LSL (Tokyo, Japan). Mouse monoclonal IgE antibody against 2,4,6-trinitrophenyl (anti-TNP IgE) was purified from the culture supernatants of a TNP-immunized mouse B lymphocyte cell line (American Type Culture Collection Number; TIB-142).

2.2. Construction of a targeting vector

Mouse genomic DNA including the A3AR gene was cloned by polymerase chain reaction (PCR) screening from bacterial artificial chromosome clones of a 129 mouse embryonic stem (ES) cells library (Genome Systems, St. Louis, MO). Human A3AR cDNA was cloned by PCR from a human liver cDNA library (Invitrogen, Carlsbad, CA). A targeting vector designed to replace the sequence coding for the mouse A3AR gene by the human A3AR cDNA sequence was generated containing the following six DNA fragments: the diphtheria toxin A fragment (DT-A) expression cassette from the pKO select DT vector (Lexicon, The Woodlands, TX) as a negative selectable marker, a 6-kb mouse genomic DNA region (from the *Sma*I site in the 5′ external sequence to immediately upstream of the *ATG* initiation codon in exon 1 of the A3AR gene), a 0.96-kb region in the human A3AR cDNA (from the *ATG* initiation codon to the *TAG* stop codon), a 0.45-kb mouse genomic DNA region (from immediately downstream of the *TAG* stop codon to the polyadenylation site in exon 2 of the A3AR gene), the *lox*P site-flanked hypoxanthine phosphoribosyltransferase (HPRT) expression cassette from the pKO select HPRT vector (Lexicon) as a positive selectable marker, and a 2.8-kb mouse genomic DNA region (from the *Bam*HI site in exon 2 to the *Apa*I site in the 3′ external sequence) (Fig. 1A).

2.3. Homologous recombination in ES cells

The targeting vector was linearized with *Sal*I and introduced into mouse ES cell line AB2.2 from the 129/SvEv strain (Lexicon) by electroporation. After selection in hypoxanthine/aminopterin/thymidine (HAT) selection medium (Lexicon), single colonies were isolated and

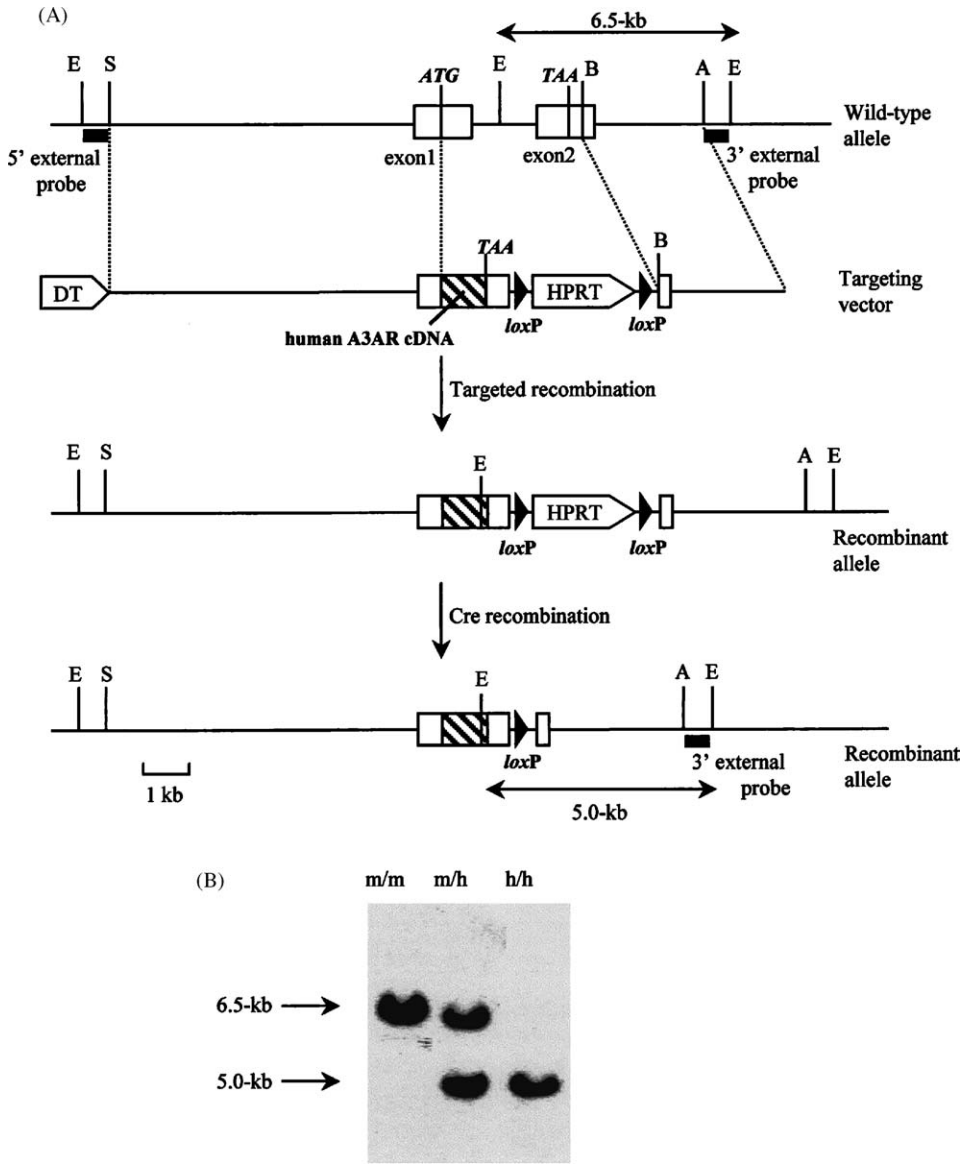

Fig. 1. Targeted replacement of mouse A3AR gene by the human gene. (A) Schematic drawing of the targeting vector and the recombinant alleles. Restriction sites *Apa*I (A), *Eco*RI (E), *Bam*HI (B), *Sma*I (S), and the location of the probe used for ES cell screening (two external probes derived from the 5′ external sequence from the *Eco*RI site to the *Sma*I site, and the 3′ external sequence from the *Apa*I site to the *Eco*RI site) and genotyping are indicated. The two exons are represented by open rectangles. The targeting vector contained a DT-A expression cassette as a negative selectable marker and an HPRT expression cassette as a positive selectable marker, and this vector replaced the region (from the *ATG* initiation codon to the *TAA* stop codon in the mouse A3AR gene) with the human A3AR cDNA sequence (from the *ATG* initiation codon to the *TAG* stop codon; striped box) by homologous recombination. The HPRT expression cassette was removed from the genomic DNA by a Cre/*lox*P recombination system. (B) Genomic Southern analysis of A3AR-humanized mice. After *Eco*RI digestion of genomic DNA purified from wild-type mice (m/m), $A3AR^{h/h}$ mice (h/h), and heterozygotes (m/h), the 3′ external probe detected a 6.5-kb band in the wild-type allele and a 5.0-kb band in the targeted allele.

verified by Southern blot analysis using two external probes derived from the 5′ external sequence from the *Eco*RI site to the *Sma*I site, and from the 3′ external sequence from the *Apa*I site to the *Eco*RI site (Fig. 1A). Identified homologous recombinant clones were transiently transfected with Cre recombinase expression vector pBS185 (Invitrogen) in order to remove the HPRT expression cassette from the recombinant allele. Clones were screened in 6-thioguanine (SIGMA) and deletion of the HPRT expression cassette was verified by Southern blot analysis using the external probes.

2.4. Generation of A3AR-humanized mice

The ES cell clones were injected into 3.5-day-old blastocysts from C57BL/6J mice (CLEA Japan, Tokyo, Japan) and were then transferred into the oviducts of pseudopregnant ICR females (CLEA Japan). The chimeric males were backcrossed to C57/BL6J mice and germ-line transmission of the mutant allele was detected by Southern blot analysis of tail-biopsy DNA from agouti offspring. Heterozygotes were intercrossed to produce homozygotes. The mice were maintained under specific pathogen-free conditions. This study

was conducted according to the Guidelines for the Care and Use of Laboratory Animals of Kyowa Hakko Kogyo Co. Ltd., in compliance with national laws and policies.

2.5. Generation of BMMCs

BMMCs were generated from femoral bone marrow cells of 8- to 10-week-old mice according to a previously described method [22]. Briefly, the cells were grown in BMMC medium, which consist of RPMI 1640 (Invitrogen) supplemented with 10% (v/v) heat-inactivated fetal bovine serum (JRH Biosciences, Lenexa, KS), 50 μM 2-mercaptoethanol (Invitrogen), 10 mg/L gentamicin (Nacalai Tesque, Kyoto, Japan), 100 μM non-essential amino acid, 100 μM sodium pyruvate, and 10% (v/v) pokeweed mitogen-stimulated spleen-conditioned medium as a source of mast cell growth factors [23], at 37 °C in a humidified atmosphere of 5% CO_2 in air. After 5 weeks, more than 95% of the non-adherent cells were identifiable as BMMCs, as determined by FACS analysis of the cell surface expression of c-kit and high-affinity IgE receptor.

2.6. Reverse transcription-polymerase chain reaction (RT-PCR)

Total RNAs were isolated from mouse tissues and BMMCs using the RNeasy kit (QIAGEN, Hilden, Germany) and single-stranded cDNAs were synthesized from 3 μg of each total RNA using the Superscript first-strand synthesis system for RT-PCR (Invitrogen) according to the manufacturer's instructions. PCR primers were synthesized for the human A3AR (sense primer 5′-AACAGCA CTG CTCTGTCATTGGCC-3′ and antisense primer 5′-TCAGA GGGATGGCAGACCACACAG-3′, which amplify a 911-bp fragment), the mouse A3AR (sense primer 5′-AACACC ACGGAGACGGACTGGCTG-3′ and antisense primer 5′-AATCTGAGGTCTGACAGAGCCTGAG-3′, which amplify a 913-bp fragment), and β-actin (sense primer 5′-GATATCGCTGCGCTCGTCGTCGAC-3′ and antisense primer 5′-CAGGAAGGAAGGCTGGAAGAGAGC-3′, which amplify a 793-bp fragment). These primers were synthesized in Proligo (Boulder, CO). PCR was carried out using TaKaRa ExTaq polymerase (TaKaRa BIO, Shiga, Japan) in GeneAmp PCR System 9700 (Perkin-Elmer, Norwalk, CT). The following PCR conditions were used for the A3AR cDNA: heating at 94 °C for 5 min and 30 subsequent cycles at 94 °C for 1 min and 68 °C for 2 min. The following PCR conditions were used for β-actin cDNA: heating at 94 °C for 5 min and 22 subsequent cycles at 94 °C for 1 min and 68 °C for 2 min. The PCR products were subjected to electrophoresis in 1.2% agarose gel for analysis.

2.7. Receptor binding assay

A saturation binding assay with the A3AR agonist [^{125}I]AB-MECA was carried out according to the method of Saki et al. [24]. Briefly, membranes of the BMMCs (100 μg) were incubated for 120 min at 25 °C with 2 U/ml adenosine deaminase and 0.0625, 0.125, 0.25, 0.5, 1.0, or 2.0 nM [^{125}I]AB-MECA in binding assay buffer (Tris–HCl buffer (50 mM, pH 7.4) containing 10 mM $MgCl_2$). The assays were performed in the presence of 1% of the final concentration of dimethyl sulfoxide, and non-specific binding was determined in the presence of 100 μM (*R*)-PIA. Binding reactions were terminated by filtration of the membranes through a MultiScreen GF/B filter (MILLIPORE, Bedford, MA). After three washes with ice-cold binding assay buffer, the radioactivity of the samples was determined using a COBRA γ-counter (Packard, Downers Grove, IL). The competitive binding assay was carried out according to the method described above (with the addition of 0.8 nM [^{125}I]AB-MECA and 0.001, 0.01, 0.1, 1.0, 10, or 100 nM KF26777).

2.8. Measurement of intracellular Ca^{2+} concentration

BMMCs were incubated in BMMC medium with saturating concentrations of anti-TNP IgE (100 ng/ml per 10^6 cells) overnight. After washing the cells twice in Ca^{2+} assay buffer (115 mM NaCl, 5.4 mM KCl, 0.8 mM $MgCl_2$, 1.8 mM $CaCl_2$, 13.8 mM glucose, 2.5 mM Probenecid, and 20 mM HEPES, pH 7.4, with 0.2%, w/v, BSA), they were incubated for 60 min at 37 °C with 5 μM Fluo-3 AM and 0.5% pluronic F-127 in the Ca^{2+} assay buffer in the dark. After the cells were washed twice in Ca^{2+} assay buffer, 2.5×10^4 cells were transferred to each well of 96-well plates and were suspended in the Ca^{2+} assay buffer at 2.5×10^5 cells/ml. After incubation for 20 min, the fluorescence intensity of Fluo-3 in each well was quantified using FDSS 6000 (Hamamatsu Photonics, Shizuoka, Japan) [25]. For measurement of the antagonist activity, the BMMCs were incubated with 100 nM KF26777 for 5 min prior to the addition of 100 nM Cl-IB-MECA. The Fluo-3 intensities were monitored every second and were plotted as a ratio against the Fluo-3 intensity at the resting calcium level. Presented data are representative of five independent experiments.

2.9. β-Hexosaminidase release assay

β-Hexosaminidase release from the BMMCs was measured according to modified versions of previously described methods [22,26]. After the anti-TNP IgE-saturated BMMCs (see above) were washed twice in phosphate buffered saline (PBS), the cells were suspended in Tyrode buffer (130 mM NaCl, 5 mM KCl, 0.6 mM KH_2PO_4, 0.6 mM $MgCl_2$, 1 mM $CaCl_2$, 0.1%, w/v, glucose, 10 mM HEPES (pH 7.4), and 0.1%, w/v, BSA) and 5×10^5 cells were transferred to 96-well plates. The cells were pre-incubated in the presence and absence of 10 nM KF26777 for 1 min prior to incubation with the indicated concentration of Cl-IB-MECA or chemokine (MIP-1α or RANTES) for 1 min at 37 °C. The cells were

stimulated with 10 ng/ml TNP-BSA for 30 min at 37 °C. The reactions were terminated by centrifugation at 2000 × *g* for 5 min at 4 °C, and the activity of β-hexosaminidase release from the BMMCs in the supernatant was assessed with *p*-nitrophenyl-*N*-acetyl-β-D-glucosaminide (SIGMA). The results were expressed as a percentage of the total Triton X-100-releasable β-hexosaminidase in whole cells.

2.10. Western blot analysis

BMMCs were stimulated by 1 μM Cl-IB-MECA at 37 °C for 0, 3, or 15 min. After two washes in ice-cold PBS, the cells were lysed in lysis buffer (62.5 mM Tris–HCl (pH 6.8), 2%, w/v, SDS, 10%, v/v, glycerol, 50 mM dithiothreitol, 0.1%, w/v, bromophenol blue) and boiled for 2 min. The cellular debris was removed by centrifugation, and the samples were resolved by SDS-polyacrylamide gel electrophoresis using e-PAGEL 5–20% (w/v) polyacrylamide gels (ATTO, Tokyo, Japan). After transfer of the proteins onto polyvinylidene difluoride membranes, protein phosphorylation was detected with rabbit phospho-specific ERK1/2, phospho-specific PKB, goat anti-rabbit horseradish peroxidase-coupled secondary antibody, and the Phototope HRP Western Blot Detection Kit. To confirm equal loading in each lane, parallel immunoblots were run in order to detect the unphosphorylated ERK1/2 and PKB using the ERK1/2 and PKB antibodies.

2.11. Internalization assay

A3AR internalization was quantified by evaluating changes in the receptor surface density after treatment of the BMMCs with 1 μM Cl-IB-MECA at 37 °C for 15 min. At the end of the incubation period, the cells were rapidly washed twice with ice-cold PBS in order to remove the Cl-IB-MECA. The amount of A3AR on the cell surface was evaluated as described above by *receptor binding assay* (with the addition of 2 nM [^{125}I]AB-MECA). The A3AR density was expressed as the percentage of total binding versus control Cl-IB-MECA-untreated cells (100%).

2.12. Data analysis

The binding parameters were calculated using Prism software (GraphPAD, San Diego, CA). The IC_{50} values obtained from the competition curves were converted to K_i values by using the Cheng and Prusoff equation [27].

3. Results

3.1. Targeted replacement of the mouse A3AR gene by its human counterpart in mice

The replacement of the mouse A3AR gene by the human A3AR cDNA was accomplished in mouse ES cells using a homologous recombination system according to the strategy shown in Fig. 1A. After electroporation of the linearized targeting vector into the mouse ES cells, HAT-resistant clones were screened by Southern blot analysis. Sixteen of the 400 clones gave bands of the expected size for the targeted allele. Four of these clones transiently expressed Cre recombinase, and removal of the HPRT expression cassette from the recombinant allele through the Cre/*lox*P recombination system in 6-thioguanine-resistant clones was ascertained by Southern blot analysis. Injection of the clones into C57BL/6J blastocysts produced 20 chimeric males exhibiting contributions from the ES cells ranging from 60 to 100%, as based on the amount of agouti coloring in the animal's coat. Four of these mice transmitted the recombinant allele through the germ line. The male chimeras were bred to C57BL/6J mice, and heterozygous offspring (A3AR$^{m/h}$ mice) were born. Homozygous mice (A3AR$^{h/h}$ mice) were obtained in crosses between A3AR$^{m/h}$ mice with the expected Mendelian inheritance. The phenotypes were detected by Southern blot analysis of tail-biopsy DNA (Fig. 1B).

3.2. Normal expression of human A3AR mRNA in A3AR$^{h/h}$ mice

Next, we measured the mRNA expression levels of human A3AR in A3AR$^{h/h}$ mice using RT-PCR analysis. The expression levels and distribution of the human A3AR mRNA in A3AR$^{h/h}$ mice were the same as those of the mouse A3AR mRNA in wild-type mice (Fig. 2). In addition, no expression of the mouse A3AR mRNA in A3AR$^{h/h}$ mice was detected (Fig. 2B).

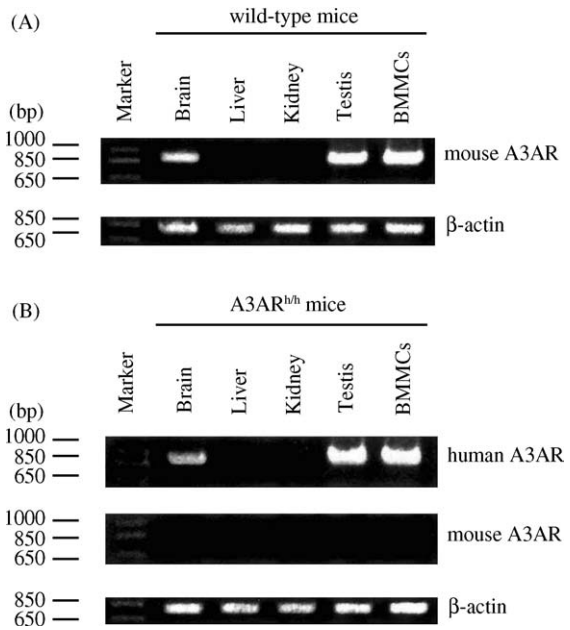

Fig. 2. Expression of human A3AR mRNA in A3AR$^{h/h}$ mice. The expression levels of mouse or human A3AR mRNA in wild-type (A) and A3AR$^{h/h}$ mice (B) were assayed using RT-PCR. The expression of β-actin mRNA was detected as a control.

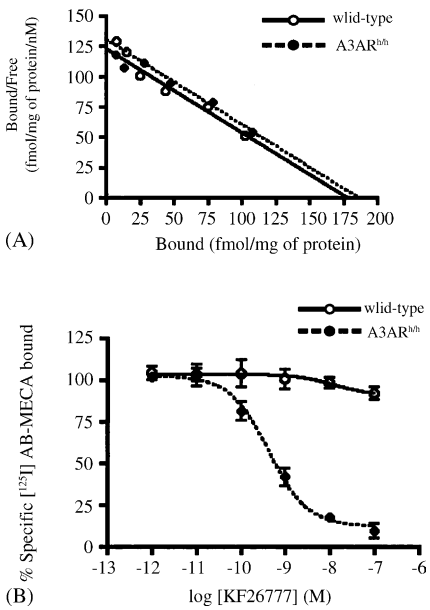

Fig. 3. Functional expression of human A3AR in BMMCs from A3AR$^{h/h}$ mice. (A) Scatchard plot for the binding of [^{125}I]AB-MECA. The K_d values were 1.45 ± 0.17 nM (wild-type mice, open circles) and 1.42 ± 0.27 nM (A3AR$^{h/h}$ mice, closed circles). The B_{max} values were 178.8 ± 11.5 and 186.2 ± 18.9 fmol/mg of protein (wild-type and A3AR$^{h/h}$ mice, respectively). (B) Competition by KF26777 for the binding of [^{125}I]AB-MECA (0.8 nM). The K_i values were >10,000 nM (wild-type mice, open circles) and 0.27 ± 0.11 nM (A3AR$^{h/h}$ mice, closed circles). Values are means ± S.D. of three experiments.

3.3. Characteristics of [^{125}I]AB-MECA binding in BMMC membranes from A3AR$^{h/h}$ mice

In order to evaluate whether or not the human A3AR was functionally expressed on mouse BMMCs, the specific and saturable binding of the A3AR agonist [^{125}I]AB-MECA was measured on membranes obtained from BMMCs (Fig. 3A). No differences were observed in terms of the A3AR density on BMMCs from A3AR$^{h/h}$ and wild-type mice (B_{max} values for BMMCs from A3AR$^{h/h}$ and wild-type mice were 186.2 ± 18.9 and 178.8 ± 11.5 fmol/mg of protein, respectively). The dissociation constant of [^{125}I]AB-MECA for the mouse A3AR on BMMCs from wild-type mice (K_d value, 1.45 ± 0.17 nM; Fig. 3A) was comparable to that for rat A3AR (K_d value, 1.46 nM [28]). The K_i value of KF26777, a human A3AR-selective antagonist, for the mouse A3AR was >10,000 nM (Fig. 3B), which is also equal to that for the rat A3AR [24]. However, the K_d value for the human A3AR on BMMCs from A3AR$^{h/h}$ mice was 1.42 ± 0.27 nM (Fig. 3A), which was two-fold lower than that in human A3AR-expressing human embryonic kidney 293 (HEK293) cells, as measured previously according to the same methods used here (0.67 ± 0.03 nM [24]). The K_i value of KF26777 for the human A3AR on BMMCs from A3AR$^{h/h}$ mice was 0.27 ± 0.11 nM (Fig. 3B), which was equivalent to that on the A3AR-expressing HEK293 cells (0.20 ± 0.038 nM [24]).

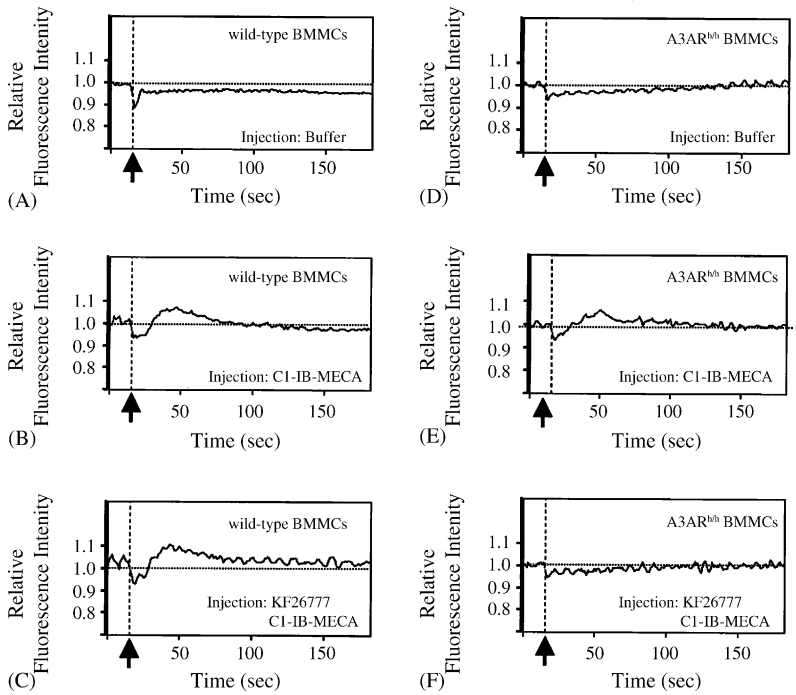

Fig. 4. The A3AR agonist induces a $[Ca^{2+}]_i$ increase in the BMMCs from A3AR$^{h/h}$ mice. BMMCs derived from wild-type (A–C) and A3AR$^{h/h}$ mice (D–F) were preloaded with Fluo-3/AM and then were stimulated with Ca^{2+} assay buffer (A and D) or 100 nM Cl-IB-MECA (B, C, E, and F). The BMMCs were pre-incubated with 100 nM KF26777 prior to the addition of Cl-IB-MECA (C and F). Fluo-3 fluorescence images were registered using FDSS 6000 system, and the relative fluorescence intensities were plotted.

3.4. The intracellular Ca^{2+} response induced by human A3AR in BMMCs from $A3AR^{h/h}$ mice

The A3AR elicits a Ca^{2+} response via heterotrimeric G proteins of the $G_{i/o}$ family [4–6]. To determine whether or not the stimulation of the human A3AR could lead to an increase in the intracellular Ca^{2+} concentration ($[Ca^{2+}]_i$) in mice, the alteration of $[Ca^{2+}]_i$ in BMMCs from $A3AR^{h/h}$ mice by a selective A3AR agonist, Cl-IB-MECA, was measured using the fluorescent Ca^{2+} indicator Fluo-3. Cl-IB-MECA was able to rapidly induce an increase in $[Ca^{2+}]_i$ in the BMMCs from wild-type and $A3AR^{h/h}$ mice (Fig. 4B and E). These $[Ca^{2+}]_i$ increases, inducing in a dose-dependent manner with saturated response of 100 nM Cl-IB-MECA, were inhibited by the pre-treatment of 200 ng/ml pertussis toxin, a inhibitor of $G_{i/o}$ proteins (data not shown). In addition, the mobilization of $[Ca^{2+}]_i$ in the BMMCs from $A3AR^{h/h}$ mice (Fig. 4F), but not in those from wild-type mice (Fig. 4C), was antagonized by KF26777. Similar results were also observed with the fluorescence indicator Fura-2 (data not shown).

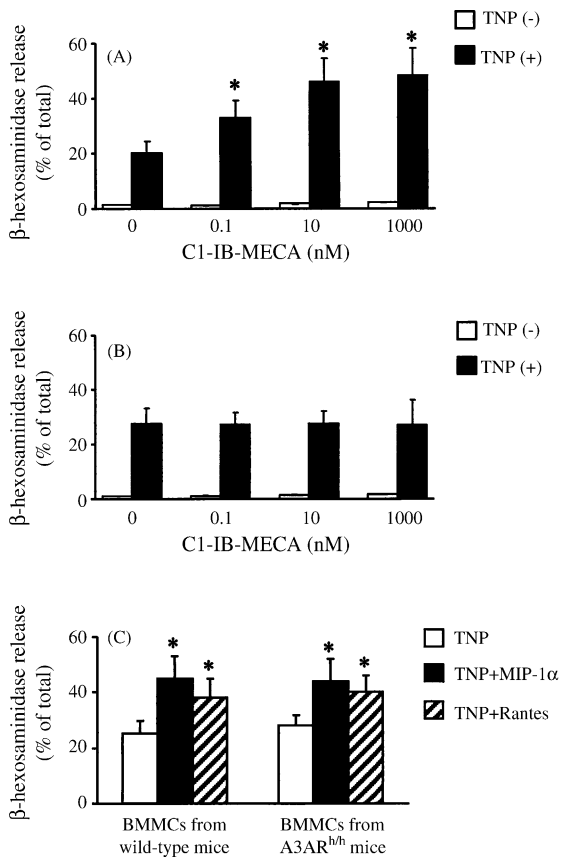

Fig. 5. No potentiation of antigen-dependent mast cell degranulation is elicited by the A3AR agonist in BMMCs from $A3AR^{h/h}$ mice. BMMCs derived from wild-type (A) and $A3AR^{h/h}$ mice (B) were pre-incubated overnight with anti-TNP IgE and then were incubated in the absence (open bars) and presence (closed bars) of antigen, 10 ng/ml TNP-BSA, for 20 min. The cells were incubated with Cl-IB-MECA (0, 0.1, 10, and 1000 nM) for 1 min prior to stimulation with the antigen. β-Hexosaminidase released in the supernatant was measured using *p*-nitrophenyl-*N*-acetyl-β-glucosaminide. (C) β-Hexosaminidase release in IgE-sensitized BMMCs from wild-type and $A3AR^{h/h}$ mice stimulated with TNP-BSA for 1 min, followed by stimulation with MIP-1α (10 nM, closed bars) or RANTES (10 nM, striped bars), is shown. Values are means ± S.E.M. from three determinations in triplicate. $^{*}p < 0.05$ compared with the values in the absence of Cl-IB-MECA (A) or MIP-1α and RANTES (C).

3.5. No potentiation of IgE/antigen-dependent degranulation by human A3AR in BMMCs from $A3AR^{h/h}$ mice

IgE/antigen-induced mast cell degranulation is strongly potentiated by A3AR via PI3Kγ [9,26]. To investigate whether or not the human A3AR mediates this response in mouse mast cells, the amount of β-hexosaminidase release [29] enhanced by Cl-IB-MECA was evaluated using IgE/antigen-stimulated BMMCs from $A3AR^{h/h}$ mice. No differences in amounts of total hexosaminidase in BMMCs from wild-type and $A3AR^{h/h}$ mice were observed (data not shown). The BMMCs from wild-type mice demonstrated a dose-dependent increase in β-hexosaminidase, as previously reported [26] (Fig. 5A). However, the BMMCs from $A3AR^{h/h}$ mice showed no such change, in comparison to stimulation with IgE/antigen alone (Fig. 5B). In mouse BMMCs, MIP-1α and RANTES, both of which are chemokine, are also known to activate PI3Kγ via chemokine receptors, and they also enhance antigen/IgE-dependent mast cell degranulation [9]. To determine whether or not PI3Kγ functions normally in the BMMCs from $A3AR^{h/h}$ mice, we investigated the changes in β-hexosaminidase release mediated by MIP-1α or RANTES via those chemokine receptors, and not via the A3AR (Fig. 5C). No significant differences in the potentiation of the IgE/antigen-dependent β-hexosaminidase release by MIP-1α or RANTES were observed between $A3AR^{h/h}$ mice and the wild-type mice.

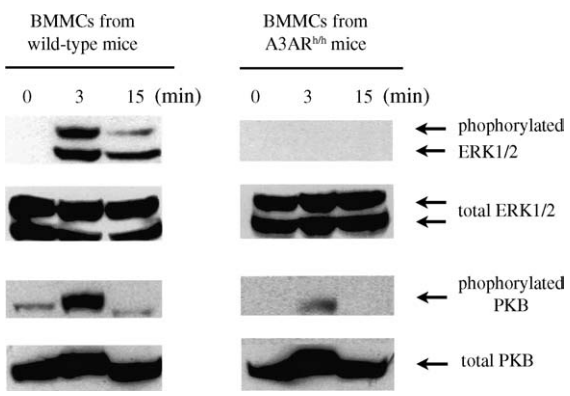

Fig. 6. No phosphorylation of ERK1/2 or PKB is induced by the A3AR agonist in BMMCs from $A3AR^{h/h}$ mice. BMMCs from wild-type (left panels) and $A3AR^{h/h}$ mice (right panels) were stimulated by 1 μM Cl-IB-MECA for 0, 3, and 15 min. The cells were washed and lysed, and then the phosphorylation of ERK1/2 and PKB was detected by Western blot analysis with anti-phosphorylated ERK1/2 or PKB antibodies. Total ERK1/2 and PKB levels were detected with anti-ERK1/2 and anti-PKB antibodies.

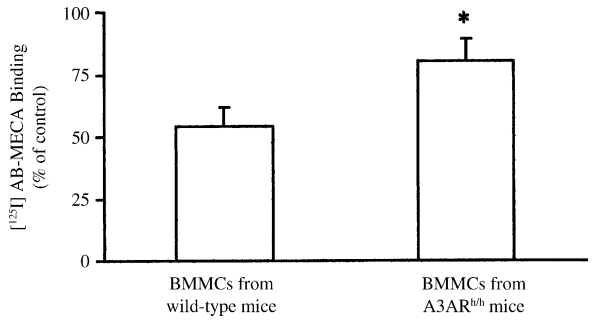

Fig. 7. The A3AR internalization induced by the A3AR agonist in BMMCs from wild-type or $A3AR^{h/h}$ mice. BMMCs were incubated with 1 μM Cl-IB-MECA at 37 °C for 15 min. After incubation, the cells were washed to remove the agonist, and the A3AR density on the cell surface was evaluated by measuring the extent of [^{125}I]AB-MECA binding for 120 min. Data are expressed as a percentage of total binding vs. control Cl-IB-MECA-untreated cells (100%). Values are mean ± S.E.M. from three determinations in triplicate. $^{*}p < 0.05$ compared with wild-type mice.

3.6. The human A3AR does not lead to the phosphorylation of either PKB or ERK1/2 in BMMCs from $A3AR^{h/h}$ mice

The A3AR is known to phosphorylate PKB and ERK1/2 in a PI3Kγ-dependent manner [4,9]. In order to evaluate whether the activation of the human A3AR leads to the phosphorylation of PKB and ERK1/2 via PI3Kγ in the BMMCs from $A3AR^{h/h}$ mice, the BMMCs stimulated by Cl-IB-MECA were subjected to immunoblotting with anti-phospho PKB and ERK1/2 antibodies. Consistent with the results of the investigation of β-hexosaminidase release, the human A3AR, when stimulated by Cl-IB-MECA, did not induce the phosphorylation of either PKB or ERK1/2 in the BMMCs from $A3AR^{h/h}$ mice, unlike in the wild-type mice (Fig. 6).

3.7. The internalization of human A3AR induced by an A3AR agonist on BMMCs from $A3AR^{h/h}$ mice

It has been reported that the phosphorylation of MAPKs, such as ERK1/2, is necessary for A3AR desensitization and internalization [30]. We therefore examined the A3AR internalization induced by Cl-IB-MECA in these BMMCs (Fig. 7). The internalization of the human A3AR in the BMMCs from $A3AR^{h/h}$ mice was significantly lower than that in the BMMCs from wild-type mice.

4. Discussion

Animal studies using rodents are essential in the field of pharmacology, especially for the early preclinical stages of drug development. However, previous studies have shown that a large number of selective agonists and antagonists for the human GPCR have reduced affinity for the rodent counterpart [31]; it has therefore remained impossible to evaluate the pharmacological effect of the targeted GPCR in rodents. In particular, the A3AR, which shows only 74% homology between human and rodent (other GPCRs usually show homology sequence ranging from 85–95%), is strongly faced with this problem [16,17]. A number of studies regarding the A3AR have demonstrated that the A3AR plays important roles in a variety of physiological process and the A3AR antagonists may be therapeutically useful for the treatment of asthma and inflammation [16–21,26]. However, the evaluation of highly potent and selective antagonists for the human A3AR using rodent animals has been hampered by the unique species specificity between the rodent and human A3AR in terms of their respective antagonist-binding affinities [17]. To overcome this problem, we generated the A3AR-humanized mice, $A3AR^{h/h}$ mice, in which the mouse A3AR gene was replaced by its human counterpart by a homologous recombination technique according to the strategy shown Fig. 1A.

To date, there have been no reports of GPCR-humanized mice, although a few generations of gene-humanized mice have been reported [32–34]. In a previous study of erythropoietin (EPO) receptor-humanized mice, it was shown that the mRNA expression of the human EPO receptor was silenced by the insertion of the expression cassette of a neomycin-resistant gene, used as a positive selection marker, in the recombinant allele [34]. For this reason, we excluded the HPRT expression cassette as a positive selection marker from the recombinant allele in ES cells using a Cre/*lox*P system. As a result, the expression levels of the human A3AR in $A3AR^{h/h}$ mice were equal to those of the mouse A3AR in wild-type mice (Figs. 2 and 3).

Next, we examined the physiological functions of the human A3AR in $A3AR^{h/h}$ mice. The agonist-mediated human A3AR elevated the $[Ca^{2+}]_i$ in BMMCs derived from $A3AR^{h/h}$ mice (Fig. 4); this elevation was completely antagonized by a highly potent and selective antagonist for the human A3AR, KF26777. However, the agonist-mediated human A3AR was unexpectedly unable to elicit the potentiation of IgE/antigen-dependent mast cell degranulation in the humanized BMMCs (Fig. 5B). To address the reason for which the human A3AR did not lead to the potentiation of mast cell degranulation, we investigated PI3Kγ activation by the human A3AR in $A3AR^{h/h}$ mice. Recent studies have demonstrated that PI3Kγ is essential for the potentiation of mast cell degranulation by the A3AR [9]. It is known that PI3Kγ is activated by the βγ subunits of some members of the $G_{i/o}$ family coupled to the A3AR, which then leads the PI3Kγ-induced phosphorylation of PKB, as well as that of members of the MAPK family, such as ERK1/2 and p38 [6,10]. Here, no human A3AR-induced phosphorylation of ERK1/2 and PKB was observed in the BMMCs from $A3AR^{h/h}$ mice (Fig. 6). Moreover, the rate of human A3AR internalization, which is known to be caused by MAPK activation [30], in the BMMCs was lower than that observed in the BMMCs from

wild-type mice (Fig. 7). However, normal PI3Kγ activity was stimulated by the chemokine MIP-1α or RANTES in the BMMCs from A3AR$^{h/h}$ mice (Fig. 5C). Taken together, these results indicated that the reduced efficacy of A3AR signaling via PI3Kγ is likely to be caused by the decreased coupling affinity between the human A3AR and the mouse $G_{i/o}$ protein(s), which activates PI3Kγ, despite the mouse G protein(s) responsible for the $[Ca^{2+}]_i$ elevation are coupled with the human A3AR. Our results therefore suggested that the A3AR uses different G proteins for the activation of PI3Kγ and for the mobilization of $[Ca^{2+}]_i$, and the $[Ca^{2+}]_i$ elevation induced by the A3AR makes no contribution to the potentiation of mast cell degranulation. The reason why the human A3AR was slightly internalized by the A3AR agonist despite no phosphorylation of ERK1/2 remains to be solved. The more detailed analysis of the human A3AR in BMMCs and/or other A3AR highly expressing tissues, such as brain and testis, will provide a new insight into the mechanism of A3AR signaling.

It is generally thought that an uncoupling of G protein from the GPCR leads to a relative reduction in the binding affinity of the ligand to the GPCR [35–37]. Our findings revealed that the binding affinity of [^{125}I]AB-MECA to the human A3AR in A3AR$^{h/h}$ mice was approximately two-fold lower than that in a human cell line (Fig. 3A); these findings thus suggest the existence of the uncoupling form of the human A3AR in A3AR$^{h/h}$ mice. It was also of note that the binding affinity of KF26777 to A3AR was unaffected by the uncoupling form (Fig. 3B) of the human A3AR, thus suggesting that the tertiary structure required for the binding of KF26777 might differ from that required for the binding of [^{125}I]AB-MECA.

It appears that the uncoupling of the mouse $G_{i/o}$ protein(s), which activates PI3Kγ, to the human A3AR is due to the low intracellular region homology between the human and mouse A3AR (only 78%). Auchampach et al. have also reported that the canine A3AR, when expressed in the African green monkey kidney cell line COS-7 or in transgenic mice, also exhibits a low-affinity state for the A3AR agonist, probably due to the decreased coupling affinity between the canine A3AR and the G protein(s) of other species [38,39]. In the case of EPO receptor-humanized mice, a reduction in the efficiency of EPO receptor signaling has been observed [34]. In order to elucidate the signaling pathways downstream of the human A3AR, most studies have taken advantage of cell lines from different species (e.g., Chinese hamster ovary cell lines). Numerous studies have shown that the human A3AR on Chinese hamster ovary cells activates the MAPK cascade via PI3Kγ, despite our hypothesis that the coupling of rodent G proteins to the human A3AR would be insufficient to activate PI3Kγ. Conceivably, this coupling may be the result of the non-physiological over-expression of the human A3AR on Chinese hamster ovary cells. Actually, lack of A3AR-induced signaling in the engineered rodent cells with low expression of human A3AR is often rescued by co-expression of human $G_{i/o}$ proteins. To settle this issue, the human/mouse chimeric A3AR, in which G protein-coupled regions of the human A3AR are exchanged with the corresponding regions of the mouse A3AR, will be analyzed.

In conclusion, we reported here for the first time the generation of mice with a replaced GPCR, i.e., the A3AR, by its human counterpart. The human A3AR led to the $[Ca^{2+}]_i$ elevation via the mouse G protein(s). However, the human A3AR did not activate the PI3Kγ signaling pathway involving the potentiation of mast cell degranulation, which was most likely due to the uncoupling of the other mouse $G_{i/o}$ protein(s) to the human A3AR. The results of the present study suggested that the replacement of the mouse A3AR with the human A3AR is insufficient to generate the A3AR-humanized mice for the functional evaluation of the human A3AR. In this context, it appears necessary to generate mice with affinities for both the human ligand and the mouse $G_{i/o}$ protein, such as those with the human/mouse chimeric A3AR; the generation of these mice is now in progress in our laboratory.

Acknowledgements

We thank Drs. Katsutoshi Sasaki, Kazumi Kurata-Miura, and Satoshi Saeki for helpful discussion.

References

[1] Olah ME, Stiles GL. Adenosine receptor subtypes: characterization and therapeutic regulation. Annu Rev Pharmacol Toxicol 1995;35:581–606.
[2] Fredholm BB, IJzerman AP, Jacobson KA, Klotz KN, Linden J. International Union of Pharmacology. XXV. Nomenclature and classification of adenosine receptors. Pharmacol Rev 2001;53:527–52.
[3] Klinger M, Freissmuth M, Nanoff C. Adenosine receptors: G protein-mediated signalling and the role of accessory proteins. Cell Signal 2002;14:99–108.
[4] Schulte G, Fredholm BB. Signaling pathway from the human adenosine A_3 receptor expressed in Chinese hamster ovary cells to the extracellular signal-regulated kinase 1/2. Mol Pharmacol 2002;62:1137–46.
[5] Englert M, Quitterer U, Klotz KN. Effector coupling of stably transfected human A_3 adenosine receptors in CHO cells. Biochem Pharmacol 2002;64:61–5.
[6] Schulte G, Fredholm BB. Signalling from adenosine receptors to mitogen-activated protein kinases. Cell Signal 2003;15:813–27.
[7] Ghosh M, Smrcka AV. Assay for G protein-dependent activation of phospholipase C β using purified protein components. Methods Mol Biol 2004;237:67–75.
[8] Stephens LR, Eguinoa A, Erdjument-Bromage H, Lui M, Cooke F, Coadwell J, et al. The Gβγ sensitivity of a PI3K is dependent upon a tightly associated adaptor, p101. Cell 1997;89:105–14.
[9] Laffargue M, Calvez R, Finan P, Trifilieff A, Barbier M, Altruda F, et al. Phosphoinositide 3-kinase γ is an essential amplifier of mast cell function. Immunity 2002;16:441–51.
[10] Hammarberg C, Fredholm BB, Schulte G. Adenosine A_3 receptor-mediated regulation of p38 and extracellular-regulated kinase ERK1/2

via phosphatidylinositol-3′-kinase. Biochem Pharmacol 2004;67: 129–34.
[11] Widmann C, Gibson S, Jarpe MB, Johnson GL. Mitogen-activated protein kinase: conservation of a three-kinase module from yeast to human. Physiol Rev 1999;79:143–80.
[12] Chan TO, Rittenhouse SE, Tsichlis PN. AKT/PKB and other D3 phosphoinositide-regulated kinases: kinase activation by phosphoinositide-dependent phosphorylation. Annu Rev Biochem 1999;68:965–1014.
[13] Zhang W, Liu HT. MAPK signal pathways in the regulation of cell proliferation in mammalian cells. Cell Res 2002;12:9–18.
[14] Franke TF, Hornik CP, Segev L, Shostak GA, Sugimoto C. PI3K/Akt and apoptosis: size matters. Oncogene 2003;22:8983–98.
[15] Roux PP, Blenis J. ERK and p38 MAPK-activated protein kinases: a family of protein kinases with diverse biological functions. Microbiol Mol Biol Rev 2004;68:320–44.
[16] Baraldi PG, Cacciari B, Romagnoli R, Merighi S, Varani K, Borea PA, et al. A_3 adenosine receptor ligands: history and perspectives. Med Res Rev 2000;20:103–28.
[17] Müller CE. Medicinal chemistry of adenosine A_3 receptor ligands. Curr Top Med Chem 2003;3:445–62.
[18] Fishman P, Bar-Yehuda S. Pharmacology and therapeutic applications of A_3 receptor subtype. Curr Top Med Chem 2003;3:463–9.
[19] Tilley SL, Tsai M, Williams CM, Wang ZS, Erikson CJ, Galli SJ, et al. Identification of A_3 receptor- and mast cell-dependent and -independent components of adenosine-mediated airway responsiveness in mice. J Immunol 2003;171:331–7.
[20] Zhong H, Shlykov SG, Molina JG, Sanborn BM, Jacobson MA, Tilley SL, et al. Activation of murine lung mast cells by the adenosine A_3 receptor. J Immunol 2003;171:338–45.
[21] Young HW, Molina JG, Dimina D, Zhong H, Jacobson M, Chan LN, et al. A_3 adenosine receptor signaling contributes to airway inflammation and mucus production in adenosine deaminase-deficient mice. J Immunol 2004;173:1380–9.
[22] Supajatura V, Ushio H, Nakao A, Okumura K, Ra C, Ogawa H. Protective roles of mast cells against enterobacterial infection are mediated by Toll-like receptor 4. J Immunol 2001;167:2250–6.
[23] Nakahata T, Spicer SS, Cantey JR, Ogawa M. Clonal assay of mouse mast cell colonies in methylcellulose culture. Blood 1982;60:352–61.
[24] Saki M, Tsumuki H, Nonaka H, Shimada J, Ichimura M. KF26777 (2-(4-bromophenyl)-7,8-dihydro-4-propyl-1*H*-imidazo[2,1-*i*]purin-5(4*H*)-one dihydrochloride), a new potent and selective adenosine A_3 receptor antagonist. Eur J Pharmacol 2002;444:133–41.
[25] Kao JP, Harootunian AT, Tsien RY. Photochemically generated cytosolic calcium pulses and their detection by fluo-3. J Biol Chem 1989; 264:8179–84.
[26] Salvatore CA, Tilley SL, Latour AM, Fletcher DS, Koller BH, Jacobson MA. Disruption of the A_3 adenosine receptor gene in mice and its effect on stimulated inflammatory cells. J Biol Chem 2000;275: 4429–34.
[27] Cheng Y, Prusoff WH. Relationship between the inhibition constant (K_i) and the concentration of inhibitor which causes 50% inhibition (IC_{50}) of an enzymatic reaction. Biochem Pharmacol 1973;22:3099–108.
[28] Li AH, Moro S, Forsyth N, Melman N, Ji XD, Jacobson KA. Synthesis, CoMFA analysis, and receptor docking of 3,5-diacyl-2,4-dialkylpyridine derivatives as selective A_3 adenosine receptor antagonists. J Med Chem 1999;42:706–21.
[29] Schwartz LB, Austen KF, Wasserman SI. Immunologic release of β-hexosaminidase and β-glucuronidase from purified rat serosal mast cells. J Immunol 1979;123:1445–50.
[30] Trincavelli ML, Tuscano D, Marroni M, Klotz KN, Lucacchini A, Martini C. Involvement of mitogen protein kinase cascade in agonist-mediated human A_3 adenosine receptor regulation. Biochim Biophys Acta 2002;1591:55–62.
[31] Watson S, Arkinstall S. The G-protein linked receptor FactsBook. London: Academic Press, 1994.
[32] Stacey A, Schnieke A, Kerr M, Scott A, McKee C, Cottingham I, et al. Lactation is disrupted by α-lactalbumin deficiency and can be restored by human α-lactalbumin gene replacement in mice. Proc Natl Acad Sci USA 1995;92:2835–9.
[33] Kitamoto T, Nakamura K, Nakao K, Shibuya S, Shin RW, Gondo Y, et al. Humanized prion protein knock-in by Cre-induced site-specific recombination in the mouse. Biochem Biophys Res Commun 1996; 222:742–7.
[34] Divoky V, Liu Z, Ryan TM, Prchal JF, Townes TM, Prchal JT. Mouse model of congenital polycythemia: homologous replacement of murine gene by mutant human erythropoietin receptor gene. Proc Natl Acad Sci USA 2001;98:986–91.
[35] Kenakin T. Efficacy in drug receptor theory: outdated concept or under-valued tool? Trends Pharmacol Sci 1999;20:400–5.
[36] Strange PG. Mechanisms of inverse agonism at G-protein-coupled receptors. Trends Pharmacol Sci 2002;23:89–95.
[37] Christopoulos A, Kenakin T. G protein-coupled receptor allosterism and complexing. Pharmacol Rev 2002;54:323–74.
[38] Auchampach JA, Jin X, Wan TC, Caughey GH, Linden J. Canine mast cell adenosine receptors: cloning and expression of the A_3 receptor and evidence that degranulation is mediated by the A_{2B} receptor. Mol Pharmacol 1997;52:846–60.
[39] Black Jr RG, Guo Y, Ge ZD, Murphree SS, Prabhu SD, Jones WK, et al. Gene dosage-dependent effects of cardiac-specific overexpression of the A_3 adenosine receptor. Circ Res 2002;91:165–72.